An Approach Based on Deep Learning for Estimating Accident Consequences of Radioactive Material Releases in Severe Accident Scenarios

Jiyeong Seo [a], Kyungho Jin [b], Sung-yeop Kim [b] Jaehyun Cho [a*]
[a] *Chung-Ang Univ., 84, Heukseok-ro, Dongjak-gu, Seoul, 06974, Republic of Korea*
[b] *Korea Atomic Energy Research Institute, Daedeok-daero 989-111, Yuseong-gu, Daejeon, 34057, Republic of Korea*
[*] *Corresponding author: jcho@cau.ac.kr*

Keywords : Deep learning, Radiological source term, Offsite consequence analysis, Risk assessment, Level 3 PSA

1. Introduction

Risk assessment plays a fundamental role in ensuring the safety and reliability of nuclear power plants (NPPs) by identifying vulnerabilities, quantifying risks, and supporting the development of appropriate mitigation strategies. In particular, the analysis of offsite radiological consequences following severe accidents has gained significant attention, especially after the Fukushima Daiichi NPP accident, which highlighted the critical importance of realistic consequence modeling and emergency preparedness [1]. Probabilistic Safety Assessment (PSA), typically divided into Levels 1, 2, and 3, is widely used for evaluating plant safety, with Level 2 PSA focusing on source term estimation and Level 3 PSA assessing radiological impacts on the surrounding population [2].

However, conventional consequence analysis using tools such as MACCS requires considerable computational resources and time, making challenges for real-time application and extensive scenario analysis. To address these limitations, this study proposes a data-driven approach using deep learning techniques to develop a surrogate model, referred to as the Accident Consequence Estimator. By analyzing the correlation between radiological source terms and offsite consequences, the model aims to enable swift and accurate estimation of population-weighted individual risk (PWIR), thereby supporting risk-informed decision-making and emergency response [3,4].

2. Methods and Results

A deep learning model was developed and evaluated for predicting radiological consequences of severe accidents. An application study was also conducted to assess the effectiveness of Severe Accident Guidelines (SAGs) in consequence mitigation.

2.1 Methodology

In this study, supervised learning-based regression analysis was conducted using a deep learning model. The input data comprised source term results generated by MAAP5 simulations for severe accident scenarios defined in Level 2 PSA, while the output data represented accident consequences resulting from the environmental release of source terms, analyzed using MACCS as part of Level 3 PSA. To perform this analysis, a deep learning regression model was developed and implemented in Python.

2.2 Deep learning model

The deep learning model was trained and tested on 658 severe accident scenarios, selected from 690 cases that account for 99% of the total accident frequency for OPR1000 [5]. The input data had a shape of (658, 2194, 26), where 2194 time steps correspond to the longest sequence among all scenarios; shorter sequences were padded for uniformity. The 26 input variables included the emission amounts of 25 major radionuclides (e.g., Xe, I, Cs, Cm), along with time information corresponding to the core exit temperature (CET) peak, which also represents the Severe Accident Management Guidelines (SAMG) entry point. The output data had a shape of (658, 1) and represented the PWIR associated with cancer fatality. Both input and output data were normalized using min-max scaling to enhance model stability and performance. A detailed overview of the dataset is provided in Table I.

Table I: Input and output data for deep learning model

	Input	Output
Description	Emission amounts of 25 major nuclides, including Xe, I, Cs, …, Cm	PWIR(Population-weighted individual risk) related to cancer fatality
Data format	Multivariate time series	Univariate single
Data shape	(658, 2194, 26)	(658, 1)
Special notes	Addition of core exit temperature (CET) maximum arrival time information	

To effectively process multivariate time-series data, a

Convolutional Neural Network (CNN) architecture was employed. Prior to model training, down sampling was applied to reduce the number of time steps from 2194 to 1097, thereby improving computational efficiency while preserving essential temporal features. In addition, positional encoding was incorporated to enhance the model performance to recognize temporal patterns, effectively expanding the input feature dimension. This technique, adapted from Transformer architectures, assigns each time step a unique positional embedding computed via sine and cosine functions, enabling the model to better capture temporal dependencies. As a result of these preprocessing steps, the final input shape for the CNN model was (1097, 39).

The overall architecture of the proposed deep learning model is summarized in Table II. The model comprises five Conv1D layers, each followed by MaxPooling1D layers, and subsequently Fully Connected (Dense) layers. The first Conv1D layer utilizes 64 filters, with the number of filters progressively reduced in subsequent layers (64 → 32 → 16 → 8 → 4), while dilation rates increase to capture multiscale temporal features. To ensure causality and prevent future data leakage, causal padding was applied in all Conv1D layers. Each convolutional layer is followed by a max pooling operation, which reduces the dimensionality of feature maps, decreases computational load, and mitigates overfitting. The resulting feature maps are flattened and passed through Dense layers comprising 256, 64, and 16 neurons, respectively, before reaching the final output layer. Additionally, a Dropout layer with a rate of 0.38 was included after the first Dense layer to further reduce the risk of overfitting and improve model generalization.

Table II: Architecture of the CNN-based deep learning model

	Layers	Output shape
Configurations	Input data	(1097, 39)
	Hidden layer 1: Conv1D	(1097, 64)
	MaxPooling 1D	(548, 64)
	Hidden layer 2: Conv1D	(548, 32)
	MaxPooling 1D	(274, 32)
	Hidden layer 3: Conv1D	(274, 16)
	MaxPooling 1D	(137, 16)
	Hidden layer 4: Conv1D	(137, 8)
	MaxPooling 1D	(68, 8)
	Hidden layer 5: Conv1D	(68, 4)
	MaxPooling 1D	(34, 4)
	Flatten layer	(136)
	Hidden layer 6: Dense	(256)
	Dropout (dropout rate = 0.38)	(256)
	Hidden layer 7: Dense	(64)
	Hidden layer 8: Dense	(16)
	Output layer	(1)
Activation function	ReLU, swish	
Optimizer	Adam optimizer (learning rate = 1.2E-04)	
Cost function	Mean squared error	

The model was trained using the Adam optimizer with an initial learning rate of 0.00012, and early stopping was applied to terminate training when the validation loss no longer improved. Additionally, ReduceLROnPlateau, a learning rate scheduler that reduces the learning rate when validation performance plateaus, was employed to dynamically adjust the learning rate and enhance training efficiency. To improve the stability and reliability of the predictions, an ensemble learning approach was adopted, wherein ten identical models were trained independently and their outputs averaged to yield the final prediction.

For model training, the dataset was partitioned into training (85%) and test (15%) sets. Within the training set, 85% of the data was used for training, while the remaining 25% was allocated for validation to assess generalization performance. This data partitioning strategy, illustrated in Fig. 1, resulted in 420 training samples, 140 validation samples, and 98 test samples. Such a structured data split was essential in minimizing overfitting and ensuring consistent predictive performance.

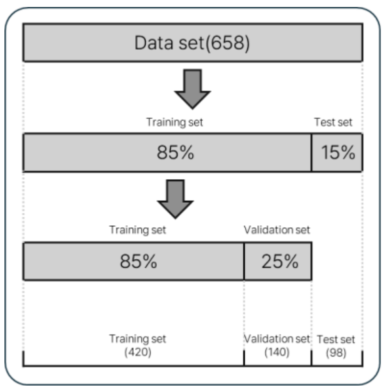

Fig. 1. Data partitioning scheme for training, validation, and testing

2.3 Model Performance Evaluation

To evaluate the predictive performance of the deep learning model, the predicted PWIR values were compared against the reference results calculated using MACCS. Fig. 2 illustrates this comparison of a randomly selected subset of 20 out of the 98 test scenarios, presented on both linear and logarithmic scales.

The model's performance was quantitatively assessed using the mean squared error (MSE), defined as:

$$MSE = \frac{1}{N}\sum_{i=1}^{N}(y_i - \hat{y}_i)^2 \quad (1)$$

where y_i denotes the true PWIR value and $\hat{y}_i$ represents the predicted value. The model achieved an MSE of approximately 0.0002, indicating a high level of agreement between the predicted and actual outcomes.

As shown in (a), the linear scale plot demonstrates that the model accurately captures the overall trend in PWIR predictions. However, due to the presence of high-fatality scenarios such as the 10th scenario, which exhibits the highest fatality rate, the PWIR values for low-fatality scenarios appear visually compressed, limiting detailed comparison. To address this issue, (b) presents the same data on a logarithmic scale, enabling more intuitive visualization across a wide range of PWIR magnitudes and improving clarity for low-fatality scenarios.

As observed from the plots, the model tends to slightly overestimate or underestimate PWIR values across different scenarios. Overestimation can lead to unnecessary conservatism in risk assessment, while underestimation may result in overlooking actual risks. Therefore, minimizing prediction errors is essential to ensure accurate risk assessment and support practical decision-making.

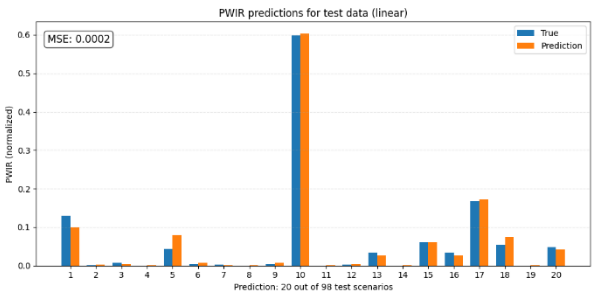

(a) Linear scale

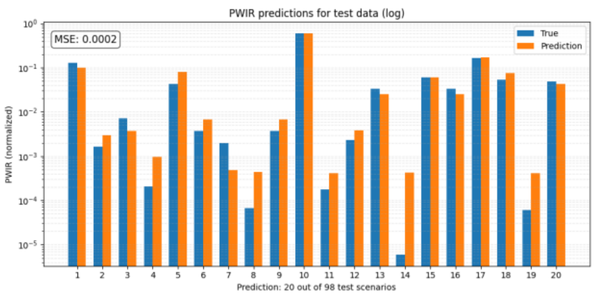

(b) Logarithmic scale

Fig. 2. PWIR predictions for 20 out of 98 test scenarios

2.4 Application study using additional SAG data

To assess the effectiveness of SAGs in mitigating radioactive release and improving accident consequences, an application study was conducted using additional SAG data. SAGs include specific Severe Accident Management (SAM) strategies aimed at preventing or mitigating severe accident phenomena. Such strategies encompass injection into the steam generators (SGs), depressurization of the reactor coolant system (RCS), injection into the RCS, injection into the containment, reduction and control of fission product (FP) release, and control of containment conditions including hydrogen concentration. Among these, SAG-01 (Injection into the SGs), SAG-02 (Depressurization of the RCS), and SAG-03 (Injection into the RCS) were selected for this study as key strategies for accident mitigation [6].

The study focused on an accident scenario corresponding to STC5, one of the Source Term Categories (STCs) defined for OPR1000, whose representative sequence is a station blackout (SBO) event. This scenario involves decay heat removal using the turbine-driven auxiliary feedwater system, with successful secondary-side heat removal. However, due to the failure of safety injection, core damage occurs, and it is assumed that the reactor containment spray system is activated within one hour after reactor vessel failure.

For analytical clarity in radionuclide release assessment, the STC5-SBO scenario without spray activation was considered as the base case (SBO, Case 0). Additional cases were established by applying different SAG strategies: Case 1 includes only SAG-01, Case 2 applies SAG-01 and SAG-02, Case 3 implements only SAG-02, Case 4 applies SAG-02 and SAG-03, and Case 5 incorporates SAG-01, SAG-02, and SAG-03 together. The configuration of each case and the corresponding SAG activation timings are summarized in Table III. A total of 16 simulations were conducted for each case by varying the SAG activation timing from 0.5 hours to 2 hours at 0.1-hour intervals, allowing for sensitivity analysis of accident mitigation effectiveness with respect to SAG implementation timing.

Fig. 3 illustrates the relative reduction in accident consequences for different SAG applications. To enhance the robustness of the predicted outcomes, each SAG dataset, although originally comprising 16 simulation cases, was processed by performing 10 independent model training iterations and reporting their ensemble average. The SBO case without any mitigation was set as the 100% baseline, and the percentage reduction in PWIR was computed for each SAG application. The results indicate that SAG-02 alone provides the highest individual effectiveness, reducing PWIR by approximately 26.3%. The combination of SAG-02 and SAG-03 achieves the greatest overall mitigation effect, reducing consequences by about 27.3%. In comparison, SAG-01 alone reduces consequences by 16.3%, and the combined application of SAG-01 and SAG-02 yields the same reduction (16.3%), indicating no additional benefit from SAG-01 when SAG-02 is applied. Interestingly, the simultaneous application of all three strategies (SAG-01, SAG-02, and SAG-03) results in a 19.1% reduction, which is lower than the effect of SAG-02 alone or in combination with SAG-03.

These findings highlight the importance of timely and appropriate SAG application in reducing the radiological impact of severe accidents. The study confirms that SAG-02 (Depressurization of the RCS) plays a crucial role in accident mitigation, and when combined with SAG-03 (Injection into the RCS), it provides the most significant consequence reduction.

Table III: Configuration of SAG application cases and activation timings

STC 5-SBO without spray	No. of simulation case	V2.SAG -01 time	V3.SAG -02 time	V4.SAG -03 time
0	1	OFF -100	OFF -100	OFF -100
1	16	ON 0.5hr-2hr	OFF -100	OFF -100
2	16	ON 0.5hr-2hr	ON 30minutes after V2	OFF -100
3	16	OFF -100	ON 0.5hr-2hr	OFF -100
4	16	OFF -100	ON 0.5hr-2hr	ON Same time with V3
5	16	ON 0.5hr-2hr	ON 30minutes after V2	ON Same time with V3

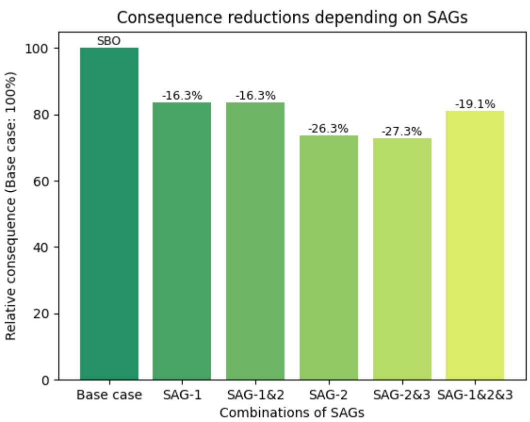

Fig. 3. PWIR(Consequence) reductions depending on SAGs

2.5 Discussion

The results presented in Fig. 3 suggest that the relationship between combinations of SAG strategies and the extent of PWIR reduction may not be strictly additive. While SAG-02 alone achieves substantial mitigation, adding SAG-01 does not appear to enhance effectiveness. In some cases, such as the combined application of all three strategies, the reduction is lower than that achieved by SAG-02 and SAG-03 together. These findings imply potential functional overlap or interference among certain SAGs, which can diminish overall effectiveness. Further investigation is needed to understand how different SAG strategies interact, complement, or counteract each other across various accident scenarios, supporting more targeted and efficient mitigation planning in severe accident management.

3. Conclusions

This study developed and evaluated a deep learning-based regression model to predict offsite radiological consequences, quantified as PWIR, based on source term data from severe nuclear accident scenarios. The model, trained using MAAP5-generated source terms and MACCS-derived consequence data, demonstrated high predictive accuracy with a mean squared error (MSE) of approximately 0.0002. Visual comparison between predicted and actual PWIR values confirmed that the model reliably captured overall trends, although slight over- or underestimations were observed across different scenarios. Based on these tendencies, minimizing prediction errors is essential to ensure accurate risk assessment and support practical decision-making.

Additionally, an application study using SAGs revealed that SAG-02 (Depressurization of the RCS) had the greatest individual effect in mitigating accident consequences. The combination of SAG-02 and SAG-03 (Injection into the RCS) achieved the highest overall reduction in PWIR, while the inclusion of SAG-01 (Injection into the SGs) offered limited additional benefit. These findings indicate that the mitigation effects of SAG combinations may not be strictly additive and highlight the need for further analysis to optimize SAG strategies based on scenario-specific effectiveness. Future research should explore these interactions across diverse accident conditions to enhance risk-informed emergency response and consequence management.

Acknowledgement

This work was supported by Korea Institute of Energy Technology Evaluation and Planning (KETEP) grant funded by the Korea government (MOTIE) (RS-2024-00401705, Convergent and practical human resource development program specialized in nuclear power plant export).

REFERENCES

[1] J.H. Lee, A. Yilmaz, R. Denning, T. Aldemir, "An online operator support tool for severe accident management in nuclear power plants using dynamic event trees and deep learning," *Ann Nucl Energy,* 146 (2020) 107626.
[2] J. Cho, S.H. Han, "Identification of Risk-Significant Components in Nuclear Power Plants to Reduce Cs-137 Radioactive Risk," *Reliab Eng Syst Saf,* 211 (2021) 107613.
[3] H. Kim, J. Cho, J. Park, "Application of a deep learning technique to the development of a fast accident scenario identifier," *IEEE Access,* 8 (2020) 177363–177373.
[4] A. Ayodeji, M.A. Amidu, S.A. Olatubosun, Y. Addad, H. Ahmed, "Deep learning for safety assessment of nuclear power reactors: Reliability, explainability, and research opportunities," *Prog Nucl Energy,* 151 (2022) 104339.
[5] K. Jin, J. Cho, S.-y. Kim, "Machine learning-based categorization of source terms for risk assessment of nuclear power plants," *Nucl Eng Technol*, 54(9) (2022) 3336–3346.
[6] J. Kim, J. Cho, S. Park, J. Park, "SAMG-based human reliability analysis method in support of Level 2 PSA. Part I: Table-top eXercise experiments," *Nucl Eng Technol,* 2024, 103375.